On the detection of a moving rigid solid in a perfect fluid

Carlos Conca, Muslim Malik, Alexandre Munnier

On the detection of a moving rigid solid in a perfect fluid

Carlos Conca*
Center for Mathematical Modelling,
University of Chile, Santiago, Chile,
Cconca@dim.uchile.cl

Muslim Malik
Center for Mathematical Modelling,
University of Chile, Santiago, Chile

Alexandre Munnier
Institut Elie Cartan UMR 7502, Nancy-Université,
CNRS, INRIA, B.P. 239,
F-54506 Vandoeuvre-lès-Nancy Cedex, France,
Alexandre.munnier@iecn.u-nancy.fr

April 2, 2010

Abstract

In this paper, we consider a moving rigid solid immersed in a potential fluid. The fluid-solid system fills the whole space and the fluid is assumed to be at rest at infinity. Our aim is to study the inverse problem, initially introduced in [3], that consists in recovering the position and the velocity of the solid assuming that the potential function is known at a given time.

We show that this problem is in general ill-posed by providing counterexamples for which the same potential corresponds to different positions and velocities of a same solid. However, it is also possible to find solids having a specific shape, like ellipses for instance, for which the problem of detection admits a unique solution.

Using complex analysis, we prove that the well-posedness of the inverse problem is equivalent to the solvability of an infinite set of nonlinear equations. This result allows us to show that when the solid enjoys some symmetry properties, it can be *partially* detected. Besides, for any solid, the velocity can always be recovered when both the potential function and the position are supposed to be known.

At last, we prove that by performing continuous measurements of the fluid potential over a time interval, we can always track the position of the solid.

1 Introduction

1.1 History

Sonars are the most common devices used to spot immersed bodies, like submarines or banks of fish. These systems use acoustic waves: active sonars emit acoustic waves (making themselves

*C. Conca thanks the MICDB for partial support through Grant ICM P05-001-F, Fondap-Basal-Conicyt, and the French & Chilean Governments through Ecos-Conicyt Grant C07E05.

detectable), while passive sonars only listen (and therefore are only able to detect targets that are noisy enough). To overcome these limitations, it would be interesting to design systems imitating the *lateral line systems* of fish, a sense organ they use to detect movement and vibration in the surrounding water.

Most of the published results on inverse problems in Fluid Mechanics concern the detection of fixed immersed obstacles. Let us mention the article [1] of Alvarez *et al*, in which the authors prove that a fixed smooth convex obstacle surrounded by a fluid governed by the Navier-Stokes equations can be identified via a localized boundary measurement of the velocity of the fluid and the Cauchy forces. In [4], the authors identify a single rigid obstacle immersed in a Navier-Stokes fluid by measuring both the gradient of the pressure and the velocity of the fluid on one part of the boundary. The distance from a given point to an obstacle is estimated in [5] from boundary measurements for a fluid governed by the stationary Stokes equations.

To our knowledge, the only work addressing the detection of moving bodies is the article [3] of Conca *et al.* In this paper, the authors consider a single moving disk in an ideal fluid and prove that the position and velocity of the body can be deduced from one single measurement of the potential along some part of the exterior boundary of the fluid. They obtain linear stability results as well, by using shape differentiation technics.

1.2 Problem settings

Domains, frames, coordinates

At a given time t, we assume that a rigid solid occupies the domain $\mathcal{S} \subset \mathbf{R}^2$, while the domain $\mathcal{F} := \mathbf{R}^2 \setminus \bar{\mathcal{S}}$ is filled by a perfect fluid. Let us assume that $\mathcal{S}$ is a simply connected compact set. The unitary normal to $\partial\mathcal{F}$ directed toward the exterior of $\mathcal{F}$ is denoted by $\mathbf{n}$. As being a rigid solid, $\mathcal{S}$ is the image by a rotation and a translation of a given reference domain $\mathcal{S}_0$ which will merely be called in the sequel the *shape* of the solid. Therefore, at any time, there exist an angle $\theta \in \mathbf{R}/2\pi$, a rotation matrix $R(\theta) \in SO_2(\mathbf{R})$ of angle θ, a point $\mathbf{s} := (s_1, s_2)^T \in \mathbf{R}^2$ (the center of the rotation) and a vector $\mathbf{r} := (r_1, r_2)^T$ of $\mathbf{R}^2$ such that $\mathcal{S} = R(\theta)(\mathcal{S}_0 - \mathbf{s}) + \mathbf{r}$. We will be concerned with recovering the position of the solid, so it is worth remarking that the triplet $(\theta, \mathbf{s}, \mathbf{r})$ is not unique. Two triplets $(\theta_j, \mathbf{s}_j, \mathbf{r}_j) \in \mathbf{R}/2\pi \times \mathbf{R}^2 \times \mathbf{R}^2$ $(j = 1, 2)$ give the same position for any $\mathcal{S}_0$ if and only if $R(\theta_1) = R(\theta_2) = R$ and $R(\mathbf{s}_1 - \mathbf{s}_2) = \mathbf{r}_1 - \mathbf{r}_2$. These equalities define an equivalence relation in $\mathbf{R}/2\pi \times \mathbf{R}^2 \times \mathbf{R}^2$. However, we want also to take into account the possible symmetries of the solid. So, given $\mathcal{S}_0$, we say that two triplets $(\theta_j, \mathbf{s}_j, \mathbf{r}_j)$ are equivalent when $R(\theta_1)(\mathcal{S}_0 - \mathbf{s}_1) + \mathbf{r}_1 = R(\theta_2)(\mathcal{S}_0 - \mathbf{s}_2) + \mathbf{r}_2$. We denote by $\mathcal{P}$ the set of all of the equivalence class $\mathbf{p}$. We will make no difference in the notation between $\mathbf{p}$ and any element $(\theta, \mathbf{s}, \mathbf{r})$ belonging to this class. In particular, we will write in short that for any $x \in \mathbf{R}^2$, $\mathbf{p}x = R(\theta)(x - \mathbf{s}) + \mathbf{r}$. In the sequel, $\mathbf{p}$ will be merely referred to as *position* of the solid.

Later on, we will use tools of complex analysis so rather than $\mathbf{R}^2$, we will sometimes identify the plane with the complex field $\mathbf{C}$. For any complex number $z := z_1 + iz_2$ ($i^2 = -1$, $z_1, z_2 \in \mathbf{R}$), we will denote $\bar{z} := z_1 - iz_2$ the conjugate of z and D will stand for the unitary disk of $\mathbf{C}$.

Sequences of complex numbers

For any sequence of complex numbers $c := (c_k)_{k\in\mathbf{Z}}$, we can define $\bar{c} := (\bar{c}_k)_{k\in\mathbf{Z}}$ and $\check{c} := (\bar{c}_{-k})_{k\in\mathbf{Z}}$. For any two sequences $a := (a_k)_{k\in\mathbf{Z}}$ and $b := (b_k)_{k\in\mathbf{Z}}$, we recall the definition of the convolution product: $a*b := (\sum_{j\in\mathbf{Z}} a_{k-j}b_j)_{k\in\mathbf{Z}}$. The convolution product can be iterated n times (n an integer) to obtain $a^n := a * a * \ldots * a$.

Rigid velocity

The solid is moving. We denote by $\mathbf{v}(x) := (v_1(x), v_2(x))^T \in \mathbf{R}^2$ the rigid Eulerian velocity field defined for all $x \in \mathcal{S}$. This notation turns out to be $v(z) := v_1(z) + iv_2(z)$ in complex notation. It is well known in Solid Mechanics that $\mathbf{v}$ can be decomposed into the sum of an instantaneous rotational velocity field and a translational velocity field. For any $x := (x_1, x_2)^T \in \mathbf{R}^2$, we introduce the notation $x^\perp := (-x_2, x_1)^T$ and we have $\mathbf{v}(x) = \omega(x - \mathbf{s})^\perp + \mathbf{w}$ where $\mathbf{s} \in \mathbf{R}^2$ is the center of the instantaneous rotation, $\omega \in \mathbf{R}$ is the angular velocity and $\mathbf{w} := (w_1, w_2)^T \in \mathbf{R}^2$ the translational velocity. Since we will be willing to recover these data, it is worth observing that the triplet $(\omega, \mathbf{s}, \mathbf{w}) \in \mathbf{R} \times \mathbf{R}^2 \times \mathbf{R}^2$ is not unique. Both triplets $(\omega_j, \mathbf{s}_j, \mathbf{w}_j)$ $(j = 1, 2)$ give the same rigid velocity field $\mathbf{v}$ if and only if $\omega_1 = \omega_2 = \omega$ and $\omega(\mathbf{s}_1^\perp - \mathbf{s}_2^\perp) = \mathbf{w}_1 - \mathbf{w}_2$ (in particular, we can always choose for $\mathbf{s}$ any point of $\mathbf{R}^2$). This is an equivalence relation and the velocity $\mathbf{v}$ can be seen as an equivalence class. We denote $\mathcal{V}$ the set of all of the equivalence class and we will make not difference, in what follows, between the vector field, the class of equivalence and any element of this class. All of them will be denoted by $\mathbf{v}$.

Definition 1.1 (Configurations)**.** For any given shape $\mathcal{S}_0$, we define a *configuration* as any position-velocity pair $(\mathbf{p}, \mathbf{v}) \in \mathcal{P} \times \mathcal{V}$.

Fluid dynamics

The dynamics of the fluid is described by means of its Eulerian velocity field $\mathbf{u}(x) := (u_1(x), u_2(x))^T$ defined for all $x \in \mathcal{F}$. Since the fluid is assumed to be perfect (i.e. incompressible and inviscid) and the flow irrotational, there exists a potential function φ, harmonic in $\mathcal{F}$, such that $\mathbf{u}(x) = \nabla\varphi(x)$ $(x \in \mathcal{F})$. The fluid is assumed to be at rest at infinity so we impose the asymptotic behavior $|\nabla\varphi(x)| \to 0$ as $|x| \to +\infty$. The classical *slip* boundary condition for inviscid fluid reads $\mathbf{u}\cdot\mathbf{n} = \mathbf{v}\cdot\mathbf{n}$ on $\partial\mathcal{S}$ and yields a Neumann boundary condition for φ, namely $\partial_n\varphi = \mathbf{v}\cdot\mathbf{n}$ on $\partial\mathcal{S}$. Although the domain $\mathcal{F}$ is not simply connected, we can still consider ψ, the harmonic conjugate function to φ, because $\int_{\partial\mathcal{S}} \partial_n\varphi \mathrm{d}\sigma = 0$. The functions φ and ψ satisfy the relation $\nabla\psi = (\nabla\varphi)^\perp$ in $\mathcal{F}$. In Fluid Mechanics, ψ is called the stream function and the complex function $\xi = \varphi + i\psi$ is the holomorphic complex potential. As usual, we define $u := u_1 + iu_2 = \bar{\xi}'$ as the complex fluid velocity. Observe that the complex potential, as being solution of a boundary value problem, depends on the domain $\mathcal{F}$ and the velocity $\mathbf{v}$ only. With the notation introduced earlier, we deduce that ξ depends only on the shape $\mathcal{S}_0$ and the configuration $(\mathbf{p}, \mathbf{v}) \in \mathcal{P} \times \mathcal{V}$.

The complex potential is defined up to an additive constant which can be chosen such that $|\xi(z)| \to 0$ as $|z| \to +\infty$. For any $\nu \in \mathbf{C}$, the complex potential can be expanded in the form of a Laurent series:

$$\xi(z) := \sum_{j\geq 1} \frac{\lambda_j(\nu)}{(z-\nu)^j}, \quad |z - \nu| > R(\nu), \tag{1.1}$$

where $\lambda_j(\nu)$ $(j \geq 1)$ are complex numbers and $R(\nu) := \limsup_{j\to+\infty} |\lambda_j(\nu)|^{1/j}$. The series is uniformly convergent on the set $\{z \in \mathbf{C} : |z - \nu| > R(\nu)\}$.

Measurements

We measure the complex velocity u of the fluid in some open subset of $\mathcal{F}$. The Analytic Continuation theorem tells us that we can deduce the value of ξ' everywhere in the connected open set $\mathcal{F}$ and then also the value of ξ, up to an additive constant. In particular, we will assume that for all $\nu \in \mathbf{C}$, we can always evaluate all of the terms of the complex sequence $(\lambda(\nu))_{j\geq 1}$ arising in the expression (1.1).

1.3 Main results

Definition 1.2 (Detectability)**.** A solid of shape $\mathcal{S}_0$ is said to be detectable if for any configuration $(\mathbf{p}, \mathbf{v}) \in \mathcal{P} \times \mathcal{V}$, the knowledge of the potential holomorphic function ξ suffices to recover the pair $(\mathbf{p}, \mathbf{v})$.

Observe that this definition makes the property of being detectable independent of the configuration: detectability is a purely geometric property of the solid. Our first result is that not all the solids are detectable:

Theorem 1.3. *For any integer $n \geq 2$, there exist a holomorphic function ξ, a shape $\mathcal{S}_0$, and n configurations $(\mathbf{p}_j, \mathbf{v}_j) \in \mathcal{P} \times \mathcal{V}$, $j = 1, \ldots, n$ satisfying $\mathbf{p}_j \neq \mathbf{p}_k$ if $j \neq k$ such that ξ is the potential of the fluid corresponding to the solid of shape $\mathcal{S}_0$ with any of the configurations $(\mathbf{p}_j, \mathbf{v}_j)$, $j = 1, \ldots, n$.*

In other words, for any integer n, there exists at least one solid that can occupy n different positions with n different velocities and for which the fluid potential is the same. This theorem shows that the result obtained in [3] for a disk can not be generalized to any solid. However, not only the disk is a detectable body:

Proposition 1.1. *Any ellipse is a detectable solid.*

Going back to the general case, it is easy to see that the holomorphic potential never admits an analytic continuation over the whole complex plane. Furthermore, for any analytic continuation of the potential inside the solid, we will prove that the locations of the singularities provide clues allowing one in many cases to determine the position of the solid. This discussion is carried out in Subection 6.1.

According to Theorem 1.3, the problem of detection is ill-posed in the general case. However, we claim that when the solid enjoys some symmetry properties, it can be *partially detected* (i.e. some but not all of the parameters among $\mathbf{r}, \alpha, \mathbf{w}, \omega$ can be deduced from the potential). The following proposition illustrates this idea:

Proposition 1.2. *If the shape of the solid is invariant under a rotation of angle $\pi/2$ then $\mathbf{r}$, $\mathbf{w}$ and $|\omega|$ can be deduced from the potential function.*

Results of this kind are made precise in Propositions 6.4 and 6.5.

Going back now to the general case, we can also try to determine less parameters with more information. For instance, we can prove:

Proposition 1.3. *For any solid with configuration $(\mathbf{p}, \mathbf{v}) \in \mathcal{P} \times \mathcal{V}$, the knowledge of both the potential function and the position $\mathbf{p}$ suffices in recovering $\mathbf{v}$.*

At last, we can also measure the potential function not only at a given instant but over a time interval. In this case, we obtain:

Theorem 1.4 (Tracking)**.** *For any solid $\mathcal{S}_0$, if we know its position at the time $t = 0$ and we perform continuous measurements of the complex potential over the time interval $[0, T]$ for some $T > 0$ then we can deduce the configuration of the solid at any time $t \in [0, T]$.*

1.4 Outline of the paper

In the next section, we provide examples of non-detectable solids and prove Theorem 1.3. In Section 3, we derive the expression of the complex potential. In Section 4, we determine all the *stealth* solids, i.e. all the solids that can move in the fluid without disturbing it. The detection of a moving ellipse is discussed in Section 5. Section 6 is split into three parts: the first one is dedicated to the study of the singularities of the potential function and the second one to its asymptotic expansion and how these results can be used for the detection problem we are dealing with. The third subsection deals with an example of detection. In Section 7 we give the proof of Theorem 1.4 and at last in Section 8, we indicate some remaining open problems.

2 Examples of Non-detectable Solids

This Section is mostly devoted to the proof of Theorem 1.3.

Expression of the stream function

Let a shape $\mathcal{S}_0$ and a configuration $(\mathbf{p}, \mathbf{v})$ be given with $\mathbf{v} = \omega(x - \mathbf{s})^\perp + \mathbf{w}$ (for some real number ω and some vector $\mathbf{s}$) and remember that $\mathcal{S} = \mathbf{p}(\mathcal{S}_0)$. Then, let us introduce $\gamma : [0, \ell[\mapsto \gamma(s) = (\gamma_1(s), \gamma_2(s))^T \in \mathbf{R}^2$ a parameterization of $\partial\mathcal{S}$ satisfying $|\gamma'(s)| = 1$ for all $s \in [0, \ell[$ ($\ell > 0$). We assume that $\partial\mathcal{S}$ is described positively (counterclockwise parameterization), we denote $\boldsymbol{\tau} = \gamma'$ (the unitary tangent vector to $\partial\mathcal{S}$) and we get $\mathbf{n} = \boldsymbol{\tau}^\perp$. We deduce that $\partial_n\varphi = -\partial_\tau\psi$ and hence that $\partial_\tau\psi(\gamma) = -w_1\gamma_2' + w_2\gamma_1' + \omega\gamma' \cdot (\gamma - \mathbf{s})$. We can integrate along $\partial\mathcal{S}$ to obtain $\psi(\gamma) = -w_1\gamma_2 + w_2\gamma_1 + (\omega/2)|\gamma - \mathbf{s}|^2 + C$ on $\partial\mathcal{S}$, where C is real constant. This Dirichlet boundary condition for the stream function reads also: $\psi(x) = -w_1x_2 + w_2x_1 + (\omega/2)|x - \mathbf{s}|^2 + C$ on $\partial\mathcal{S}$. In this form, the boundary of the solid turns out to be a level set of the function $g(x) := (\omega/2)|x - \mathbf{s}|^2 - w_1x_2 + w_2x_1 - \psi(x)$, an observation we will now take advantage of.

Proof of Theorem 1.3

Pick some integer $n \geq 2$ and consider the harmonic function whose expression in polar coordinates is $\psi(r, \theta) := \cos(n\theta)r^{-n}$. Since, in Cartesian coordinates, $|(\partial\psi/\partial x_j)(x)| \leq |\nabla\psi(x)| = n|x|^{-n-1}$ ($j = 1, 2$), we deduce that for any $\omega > 0$ and $\mathbf{s} \in \mathbf{R}^2$, there exists $\delta > 0$ such that $(\partial\psi/\partial x_1)(x) - \omega(x_1 - s_1)$ and $(\partial\psi/\partial x_2)(x) - \omega(x_2 - s_2)$ can not be simultaneously null providing $|x - \mathbf{s}| > \delta$. Applying the local inversion Theorem, we deduce that for any $\lambda \in \mathbf{R}$, the solutions of

$$\frac{\omega}{2}|x - \mathbf{s}|^2 - \psi(x) - \lambda = 0, \tag{2.1}$$

satisfying $|x - \mathbf{s}| > \delta$ (if any) are locally smooth curves.

From the estimate $|\psi(x)| < |x|^{-n}$ ($x \in \mathbf{R}^2$), we deduce that for all $\mathbf{s} := (s_1, s_2)^T$, all $\omega > 0$ and all $\varepsilon > 0$, there exists $\delta' > 0$ such that:

$$\frac{\omega - \varepsilon}{2}|x - \mathbf{s}|^2 - \lambda \leq \frac{\omega}{2}|x - \mathbf{s}|^2 - \psi(x) - \lambda \leq \frac{\omega + \varepsilon}{2}|x - \mathbf{s}|^2 - \lambda,$$

for all $\lambda \in \mathbf{R}$ providing $|x - \mathbf{s}| \geq \delta'$. If we choose for instance $\lambda > \max(\delta', \delta)^2(\omega + \varepsilon)$, there is a zero level set of the function $g(x) := \omega|x - \mathbf{s}|^2/2 - \psi(x) - \lambda$ between the circles $|x - \mathbf{s}| = \sqrt{2\lambda}/\sqrt{\omega - \varepsilon}$ and $|x - \mathbf{s}| = \sqrt{2\lambda}/\sqrt{\omega + \varepsilon}$ (because $\sqrt{2\lambda}/\sqrt{\omega + \varepsilon} \geq \sqrt{2}\delta > \delta$). It remains to choose $\mathbf{s}$ properly, in order to take advantage of the symmetry of the function ψ. Let ρ be any positive number and denote $\mathcal{S}_1$ the zero level set of g obtained as described above by specifying $\mathbf{s}_1 := (\rho, 0)$. This level set defines the smooth boundary of a solid for which ψ is the stream function (and $\xi(z) := i/z^n$ the holomorphic potential) associated with the velocity $\mathbf{v}_1 := \omega(x - \mathbf{s}_1)^\perp$. By choosing next $\mathbf{s}_k = (\rho\cos(2(k-1)\pi/n), \rho\sin(2(k-1)\pi/n))^T$ for $k = 2, \ldots, n$, we obtained $n - 1$ copies of $\mathcal{S}_1$ at $n - 1$ different positions with respective velocities $\mathbf{v}_k := \omega(x - \mathbf{s}_k)^\perp$. Some examples of such solids with the associated rigid velocity fields are pictured in Figures 1, 2 and 3.

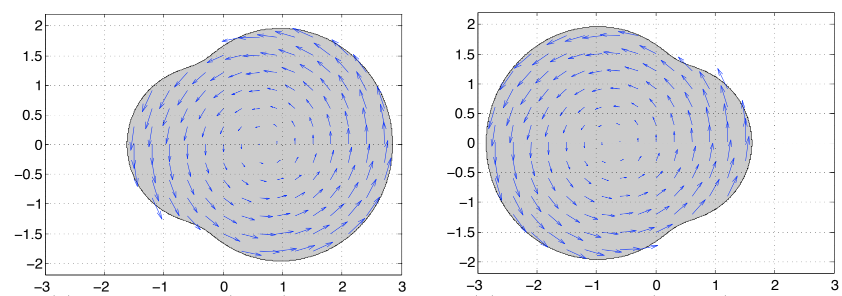

(a) $\omega = 0.7$, $\mathbf{s}_1 = (0.7, 0)$, $\lambda = 1.5$ (b) $\omega = 0.7$, $\mathbf{s}_2 = (-0.7, 0)$, $\lambda = 1.5$

Figure 1: For both configurations, the stream function is the same. It reads $\psi(r, \theta) := \cos(2\theta)/r^2$ in polar coordinates. The holomorphic potential is $\xi(z) := i/z^2$.

3 The Complex Potential

Before going further, we need to describe the shape $\mathcal{S}_0$. Actually, for convenience, rather than $\mathcal{S}_0$ we shall describe $\mathcal{F}_0 := \mathbf{C} \setminus \bar{\mathcal{S}}_0$. Thus, assume that $\mathcal{F}_0$ is the image by a conformal mapping f of $\Omega := \mathbf{C} \setminus \bar{D}$, the exterior of the unitary disk. For any simply connected shape $\mathcal{S}_0$ and corresponding domain $\mathcal{F}_0$, the Riemann mapping Theorem tells us that f can be written in the form:

$$f(z) = c_1 z + c_0 + \sum_{k \leq -1} c_k z^k, \quad (z \in \Omega), \tag{3.1}$$

where $c_k \in \mathbf{C}$ for $k = 1$ and all $k \leq -1$ and $c_1 \neq 0$. We can assume, without loss of generality, that $c_0 = 0$. To simplify forthcoming computations, we will also assume that c_k is actually defined for all $k \in \mathbf{Z}$ and that $c_k = 0$ for $k = 0$ and $k \geq 2$. We denote $c := (c_k)_{k \in \mathbf{Z}}$ the complex sequence of elements c_k and the *area Theorem* (see [7, Theorem 14.13]) tells us that the area of $\mathcal{S}_0$ is equal

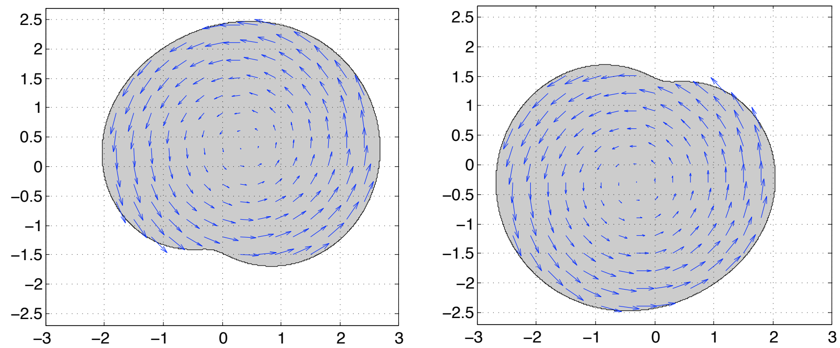

(a) $\omega = 0.6$, $\rho = 0.5$, $\lambda = 1.5$ and $\mathbf{s}_1 = (\rho\cos(\pi/4), \rho\sin(\pi/4))$

(b) $\omega = 0.6$, $\rho = 0.5$, $\lambda = 1.5$ and $\mathbf{s}_2 = (\rho\cos(-\pi/4), \rho\sin(-\pi/4))$

Figure 2: For both configurations, the stream function and the holomorphic potential are the same as in Figure 1.

to $\pi\sum_{k\leq 1} k|c_k|^2$. Since $\mathcal{S}_0$ is of finite extend, it means that this sum has to be finite. Actually, we will assume also that $c \in \ell^1(\mathbf{C})$, which entails in particular that f is continuous in the closed set $\bar{\Omega}$.

Such a description allows us to consider a broad set of solids. In particular, the boundary of the solid can be very rough. Degenerate cases can be considered as well (for instance $\mathcal{S}_0$ can be a segment modeling a one dimensional beam).

For any position $\mathbf{p} := (R(\alpha), 0, \mathbf{r})$, we recall that $\mathcal{S} := R(\alpha)\mathcal{S}_0 + \mathbf{r}$ is the actual domain occupied by the solid. Let us introduce then the functions $\varphi_0(x) := \varphi(R(\alpha)x + \mathbf{r})$ and $\psi_0(x) := \psi(R(\alpha)x + \mathbf{r})$ which are harmonic (and defined) over the fixed domain $\mathcal{F}_0$. For any velocity $\mathbf{v} := (\omega, \mathbf{r}, \mathbf{w})$ (we choose here $\mathbf{s} = \mathbf{r}$), the Dirichlet boundary condition for ψ turns out to be, with complex notation $2i\psi_0 := w_0\bar{z} - \bar{w}_0 z + i\omega|z|^2$ where $w_0(z) := w(R(\alpha)z + \mathbf{r})$. We introduce ζ the holomorphic complex potential of the fluid defined for any $z \in \Omega$ by $\zeta(z) = \varphi_0(f(z)) + i\psi_0(f(z))$. Since $\bar{z} = 1/z$ on $\partial\Omega$, we get the identity $2i\psi_0(f(z)) = -\bar{w}f(z) + w\bar{f}(1/z) + i\omega f(z)\bar{f}(1/z)$. For any $z \in \partial\Omega$, we have also $\bar{f}(1/z) = \sum_{k\in\mathbf{Z}} \bar{c}_{-k}z^k = \sum_{k\in\mathbf{Z}} \check{c}_k z^k$ and $f(z)\bar{f}(1/z) = \sum_{k\in\mathbf{Z}}(\check{c} * c)_k z^k$. So we get:

$$2i\psi_0(f(z)) = \sum_{k\in\mathbf{Z}}[-\bar{w}_0 c_k + w_0\check{c}_k + i\omega(\check{c} * c)_k]z^k, \quad (z \in \partial\Omega). \tag{3.2}$$

According to [6, Chap. IX, §9.63], we keep only the negative powers in (3.2) to get the expression of ζ. Defining the coefficients $\zeta_k(w_0, \omega) := [-\bar{w}_0 c_k + w_0\check{c}_k + i\omega(\check{c} * c)_k]$ for all $k \leq -1$, we obtain:

$$\zeta(z) = \sum_{k\leq -1} \zeta_k(w_0, \omega)z^k, \quad (z \in \Omega). \tag{3.3}$$

Eventually, the expression of the measured complex potential, defined in $\mathcal{F}$, is:

$$\xi(z) = \zeta(f^{-1}((z - r)e^{-i\alpha})), \quad (z \in \mathcal{F}). \tag{3.4}$$

According to our rule of notation, we introduce as well

$$\xi_0(z) = \varphi_0(z) + \psi_0(z) = \zeta(f^{-1}(z)), \quad (z \in \mathcal{F}_0). \tag{3.5}$$

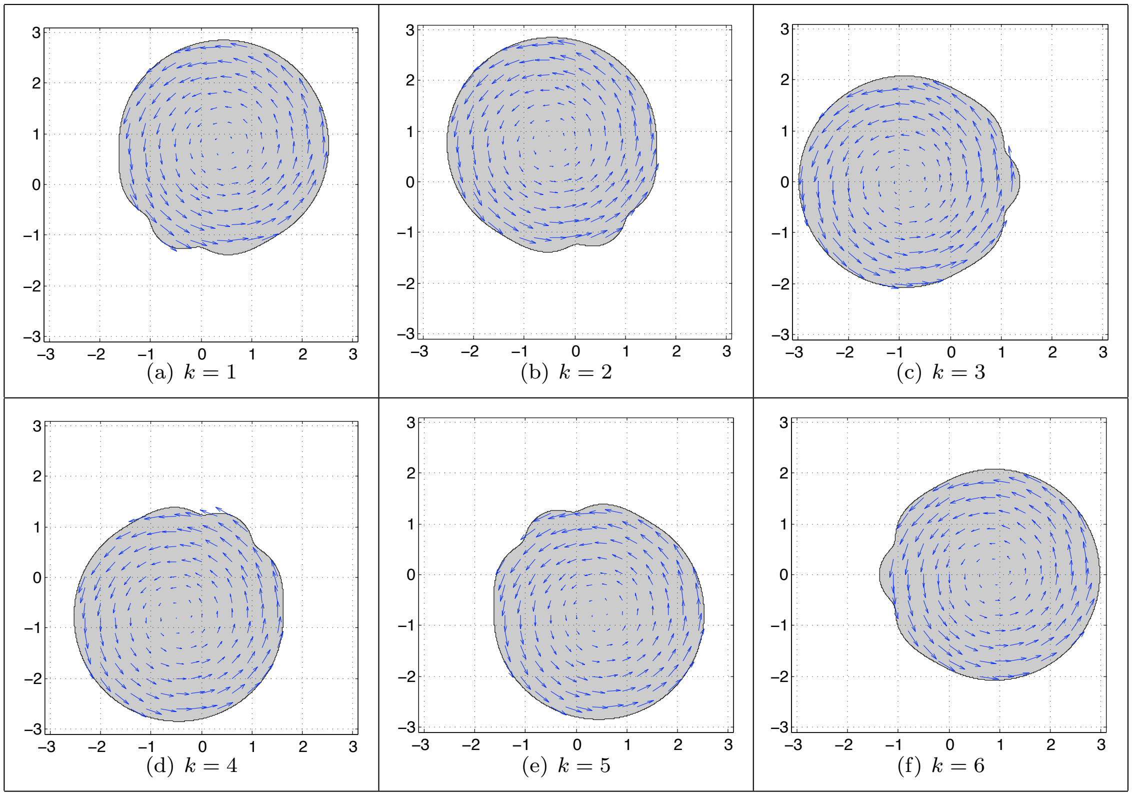

Figure 3: The stream function is $\psi(r,\theta) = \cos(6\theta)/r^6$, the holomorphic potential is $\xi = i/z^6$ and $\omega = 0.7$, $\rho = 0.9$, $\lambda = -2.5$ and $\mathbf{s}_1 = (\rho\cos(k\pi/6), \rho\sin(2k\pi/6))$ for $k = 1, \ldots, 6$.

4 Stealth Rigid Solids

In this Section we are willing to determine all the possible shapes and configurations of solids for which the complex potential ξ is identically null. Such a displacement will be termed *stealth*.

Theorem 4.1. *The only solids $\mathcal{S}$ that can undergo stealth motions in a fluid are:*

- *Disks rotating about their centers;*
- *Arc of circles and segments with velocity field everywhere tangent to $\mathcal{S}$.*

The arc of circles and segments are one dimensional solids and can be considered as degenerated cases.

Proof. Let us assume that $\xi = 0$. Then we have also $\zeta = 0$ which means that $-2\Im(\bar{u}f(z)) + \omega|f(z)|^2 = 0$ for all $z \in \partial\Omega$. If $\omega \neq 0$, some easy computations tell us that for all $z \in \partial\Omega$, $f(z)$ belongs to the circle of center $iw_0/2\omega$ and radius $|w_0|/(2|\omega|)$. Since f is an homeomorphism from $\partial\Omega$ onto $f(\partial\Omega)$, $f(\partial\Omega)$ is a connected compact subset of this circle.

- If $f(\partial\Omega)$ is the complete circle, it means that $c_1 = 1$ and $c_k = 0$ for all $k \neq 1$. In this case, since $\zeta_1 = 0$ and $(\check{c} * c)_1 = 0$, we deduce that $w_0 = 0$ and hence that the circle is just rotating about its center.
- Up to a translation and a rotation, all the conformal mappings that map the circle onto an arc of circle have the form $f(z) = z + (1-h^2)/(z+ih)$ where h is any real number such that $0 < h < 1$. We can put f into the general form (3.1) by setting: $c_1 = 1$, $c_{-1} = 1 - h^2$ and $c_k = (1-h^2)(-ih)^{-k-1}$ for all $k \leq -2$. Some simple computations lead to: $(\check{c}*c)_{-1} = -ihc_{-1}$ and $(\check{c}*c)_k = (ih^{-1} - ih)c_k$ for all $k \leq -2$. Plugging these expressions into (3.3) and writing that $\zeta_k(w_0, \omega) = 0$ for all $k \leq -1$ we obtain the same equation for all k which yields the relation: $w_0 = \omega(h - 1/h)$. We can then easy prove that this motion corresponds to the case where the velocity field is tangent to the solid.

Let us assume now that ω is zero (and $w_0 \neq 0$). In this case, we deduce with (3.3), that $c_k = 0$ for all $k \leq -2$. For $k = -1$, we get $c_{-1} = \bar{c}_1 w_0/\bar{w}_0$. We set $w_0 = Re^{i\theta}$, $c_1 = \tilde{R}e^{i\beta}$ and we rewrite f in the form:

$$f(z) = \tilde{R}\left[e^{i\beta}z + e^{i(-\beta+2\theta)}/z\right] = 2\tilde{R}e^{i\theta}\left[e^{i(\beta-\theta)}z + e^{-i(\beta-\theta)}/z\right].$$

We seek the image of the unitary circle by f. We specify $z = e^{it}$ with $t \in \mathbf{R}/2\pi$ and we get $f(e^{it}) = 2\tilde{R}e^{i\theta}\cos(\beta - \theta + t)$. So the image of the unitary circle is the segment $[-\tilde{R}, \tilde{R}]$ turned by an angle θ. The velocity w_0 is collinear to the segment. □

5 Detection of a Moving Ellipse

When $\mathcal{S}_0$ is an ellipse, the function f has the form $f(z) = (a+b)z/2 + (a-b)/2z$ where $a, b \in \mathbf{R}_+$, $a > b > 0$. We can now give the proof of Proposition 1.1.

Proof. First, we can explicitly compute the inverse function

$$f^{-1}(z) = \frac{z}{(a+b)}\Big(1 + \sqrt{1 - \frac{(a^2-b^2)}{z^2}}\Big), \quad (z \in \mathcal{F}_0). \tag{5.1}$$

In this expression, $-\sqrt{a^2-b^2}$ and $\sqrt{a^2-b^2}$ are branch points and the function is holomorphic everywhere but on the segment $[-\sqrt{a^2-b^2}, \sqrt{a^2-b^2}]$ which is a branch cut. Next, we get:

$$\zeta(z) = \Big[-\bar{w}_0\frac{a-b}{2} + w_0\frac{a+b}{2}\Big]\frac{1}{z} + i\omega\frac{a^2-b^2}{4}\frac{1}{z^2}, \quad (z \in \Omega),$$

and then:

$$\xi(z) = \frac{[-(a^2-b^2)\bar{w}_0 + (a+b)^2 w_0]e^{i\alpha}}{2(z-r)\Big[1 + \sqrt{1 - \frac{(a^2-b^2)e^{2i\alpha}}{(z-r)^2}}\Big]} + \frac{i(a^2-b^2)(a+b)^2 e^{2i\alpha}\omega}{4(z-r)^2\Big[1 + \sqrt{1 - \frac{(a^2-b^2)e^{2i\alpha}}{(z-r)^2}}\Big]^2}, \quad (z \in \mathcal{F}).$$

Observe that, owning to the symmetry of the ellipse, we can change α into $\alpha + \pi$ and accordingly w_0 into $-w_0$ without changing the expression of ξ. The potential ξ is holomorphic everywhere but on the branch cut $[r - \sqrt{a^2-b^2}e^{i\alpha}, r + \sqrt{a^2-b^2}e^{i\alpha}]$. So if we know thoroughly ξ, we can determine the location of the branch points $r - \sqrt{a^2-b^2}e^{i\alpha}$ and $r + \sqrt{a^2-b^2}e^{i\alpha}$ and hence also the position of the center r and the orientation α (up to π only). We compute next the limit $\mu := \lim_{|z|\to+\infty} e^{-i\alpha}\xi(z)z/(a+b) = [-(a-b)\bar{w}_0 + (a+b)w_0]/4$ and we deduce the expression of w_0, namely: $w_0 = (\mu+\bar{\mu})/b + (\mu-\bar{\mu})/a$. The only remaining unknown quantity ω is next easily obtained, following the same idea. □

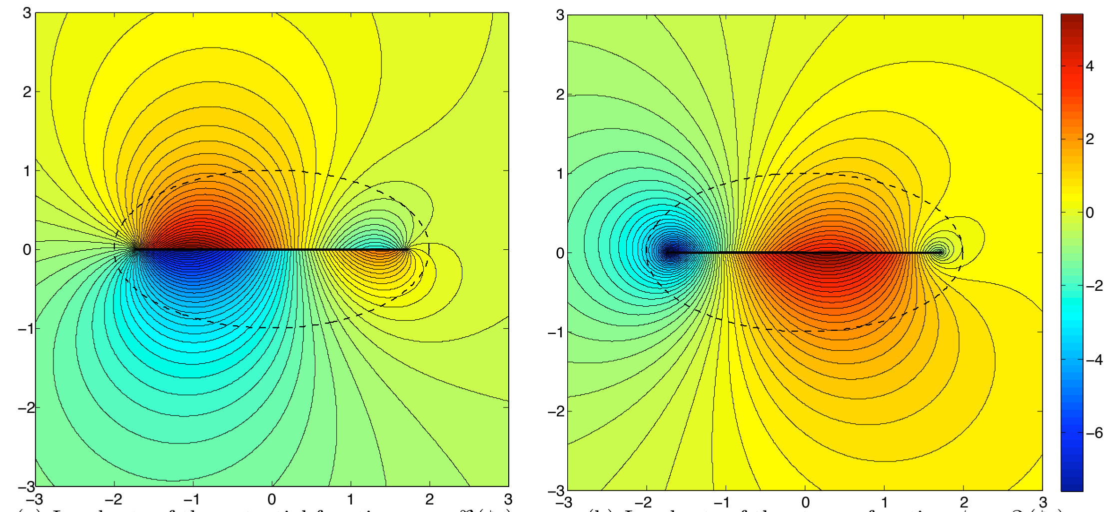

Figure 4: Level sets of the holomorphic potential ξ_0, for $a = 2$, $b = 1$, $w_0 = e^{i\pi/3}$ and $\omega = -2$. The boundary of the ellipse (dashed line) can hardly be directly detected but the branch points $-\sqrt{3}$ and $\sqrt{3}$ are easily spotted.

6 Detection: General Case

6.1 Singularities of the holomorphic potential

In the preceding example, the branch points of the potential ξ played a crucial role in determining the position of the solid in the fluid. Notice that the existence of these points did not depend on the configuration but only on the shape of the solid (they came out in the definition (5.1) of the inverse function f^{-1} and were subsequently just translated and rotated according to the position). We shall prove that this result can be generalized to any solid: there is no singularity in the potential function, that does not come from the conformal mapping f^{-1} (but unfortunately, the potential function may have less singular points than the function f^{-1}). Let us make this statement precise:

Definition 1 (Analytic continuation)**.** *An holomorphic function $\tilde{\xi}$ (repect. $\tilde{\xi}_0$) defined in a connected open set $\widetilde{\mathcal{F}}$ (respect. $\widetilde{\mathcal{F}}_0$) containing $\mathcal{F}$ (respect. $\mathcal{F}_0$) is called an analytic continuation of ξ (respect. ξ_0) when $\tilde{\xi} = \xi$ in $\mathcal{F}$ (respect. $\tilde{\xi}_0 = \xi_0$ in $\mathcal{F}_0$).*

It may exist several analytic continuations of ξ that do not coincide everywhere. Assume that $\tilde{\xi}_1$ and $\tilde{\xi}_2$ are two such functions defined respectively on $\widetilde{\mathcal{F}}_1$ and $\widetilde{\mathcal{F}}_2$. So the Analytic Continuation

Theorem ensures only that $\tilde{\xi}_1 = \tilde{\xi}_2$ on the connected component of $\widetilde{\mathcal{F}}_1 \cap \widetilde{\mathcal{F}}_2$ containing $\mathcal{F}$. In Section 5 for instance, we can not choose where the branch points are but there are many different possible choices for the branch cut, each one corresponding to a different analytic continuation of ξ.

Assume that for some potential function ξ, there exists an analytic continuation $\tilde{\xi}$ such that $\widetilde{\mathcal{F}} = \mathbf{C}$. Since, by construction, $\xi(z)$ tends to 0 as $|z|$ goes to infinity, $\tilde{\xi}$ is a bounded entire function. According to Liouville's Theorem, this function is constant, equal to 0. This case was treated in Section 4 and is possible only for solids listed in Theorem 4.1. For all of the other solids and for any analytic continuation $\tilde{\xi}$, there exists at least one point, located inside the solid, which does not belong to $\widetilde{\mathcal{F}}$. This very simple observation allows one to locate the solid in a very first approximation.

Let us now prove that the singularities of $\tilde{\xi}$ come from the singularities of f^{-1}.

Proposition 6.1. *If there exists an analytic continuation $\tilde{g}$ of f^{-1} defined on an open connected set $\widetilde{\mathcal{F}}_0$ containing $\mathcal{F}_0$, then for any configuration $(\mathbf{p}, \mathbf{v}) \in \mathcal{P} \times \mathcal{V}$, there exists an analytic continuation $\tilde{\xi}$ of ξ defined on $\widetilde{\mathcal{F}} := \mathbf{p}\big(\widetilde{\mathcal{F}}_0 \setminus \tilde{g}^{-1}(\{0\})\big)$.*

In this proposition, the notation $\tilde{g}^{-1}(\{0\})$ stands for the preimage of $\{0\}$ under $\tilde{g}$ and does not mean that $\tilde{g}$ is invertible. Since $\tilde{g}$ is holomorphic, the set $\tilde{g}^{-1}(\{0\})$ consists only in isolated points and $\widetilde{\mathcal{F}}_0 \setminus \tilde{g}^{-1}(\{0\})$ is still connected and still contains $\mathcal{F}_0$.

Proof. For all $z \in \partial D$, we can rewrite ζ in the form:

$$\zeta(z) = -\bar{w}_0(f(z) - c_1 z) + w_0 \bar{c}_1 z^{-1} + i\omega\Big[\bar{c}_1 z^{-1}(f(z) - c_1 z) + \sum_{k \geq 1} \bar{c}_{-k} z^k \Big(f(z) - \sum_{-k \leq j \leq 1} c_j z^j\Big)\Big]. \quad (6.1)$$

Expanding the right hand side and recombining terms, we get the identity:

$$\zeta(z) = -\bar{w}_0 f(z) + c_1 \bar{w}_0 z + u\bar{c}_1 z^{-1} + i\omega\Big[f(z)\bar{f}(z^{-1}) - H_1(z)\Big], \quad (z \in \partial D),$$

where $H_1(z) := \sum_{j \geq 0} (\check{c} * c)_j z^j$ and $\bar{f}(z) := \bar{c}_1 z + \sum_{k \leq -1} \bar{c}_k z^k$. Classical results for the convolution product ensure that this series is uniformly convergent for $|z| \leq 1$ since $\|\check{c} * c\|_{\ell^1(\mathbf{C})} \leq \|\check{c}\|_{\ell^1(\mathbf{C})} \|c\|_{\ell^1(\mathbf{C})}$. We next obtain that:

$$\zeta(f^{-1}(z)) = -\bar{w}_0 z + c_1 \bar{w}_0 f^{-1}(z) + u\bar{c}_1 / f^{-1}(z) + i\omega\Big[z\bar{f}(1/f^{-1}(z)) - H_1(f^{-1}(z))\Big], \quad (z \in \partial\mathcal{S}_0).$$

Let $\tilde{g}$ by any analytic continuation of f^{-1} (not necessary invertible), defined in an open set $\widetilde{\mathcal{F}}_0$. It can be split into three parts: $\widetilde{\mathcal{F}}_0^+ := \{z \in \widetilde{\mathcal{F}}_0 \,:\, |\tilde{g}(z)| > 1\}$, $\widetilde{\mathcal{F}}_0^- := \{z \in \widetilde{\mathcal{F}}_0 \,:\, 0 < |\tilde{g}(z)| < 1\}$ and $\widetilde{\mathcal{F}}_0^1 := \{z \in \mathbf{C} \,:\, \tilde{g}(z) = 1\}$. We can next define:

$$\begin{aligned}
\tilde{\xi}_0(z) &:= -\bar{w}_0 z + c_1 \bar{w}_0 \tilde{g}(z) + w_0 \bar{c}_1 / \tilde{g}(z) + i\omega\Big[z\bar{f}(1/\tilde{g}(z)) - H_1(\tilde{g}(z))\Big], \quad && z \in \widetilde{\mathcal{F}}_0^- \cup \widetilde{\mathcal{F}}_0^1, \\
\tilde{\xi}_0(z) &:= -\bar{w}_0 z + c_1 \bar{w}_0 \tilde{g}(z) + w_0 \bar{c}_1 / \tilde{g}(z) + i\omega\Big[H_2(\tilde{g}(z))\Big], && z \in \widetilde{\mathcal{F}}_0^+,
\end{aligned}$$

where $H_2(z) := \sum_{j \leq -1} (\check{c} * c)_j z^j$ is uniformly convergent for $|z| \geq 1$. We deduce that the function $\tilde{\xi}_0$ is holomorphic in $\widetilde{\mathcal{F}}_0^-$ and in $\widetilde{\mathcal{F}}_0^+$ and continuous in $\widetilde{\mathcal{F}}_0 \setminus \tilde{g}^{-1}(\{0\})$. Let $z_0 \in \widetilde{\mathcal{F}}_0^1$ and denote

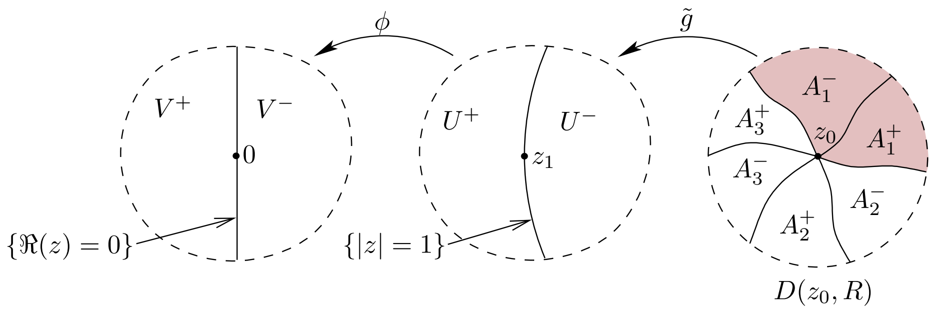

Figure 5: The conformal mapping $\tilde{g}$ nearby the point z_0 for $n = 3$.

$z_1 := \tilde{g}(z_0)$. Since $\tilde{g}$ is holomorphic at the point z_0, there exist $R > 0$, $n \geq 1$ and a function h holomorphic in the disk $D(0, R)$ such that $h(0) \neq 0$ and

$$\tilde{g}(z) = z_1 + (z - z_0)^n h(z - z_0), \quad z \in D(0, R).$$

This identity allows us to describe the set $\widetilde{\mathcal{F}}_0^1$ nearby the point z_0. For instance, if $n = 3$, and for R small enough, we get something like in Figure 5 where $z_1 = \tilde{g}(z_0)$, $\cup_{j=1}^3 A_j^+ = D(z_0, R) \cap \widetilde{\mathcal{F}}_0^+$, $\cup_{j=1}^3 A_j^- = D(z_0, R) \cap \widetilde{\mathcal{F}}_0^-$ and the curves radiating from z_0 correspond to the set $D(z_0, R) \cap \widetilde{\mathcal{F}}_0^1$. Except maybe at the point z_0, the boundaries shared by the regions A_j^+ and A_j^- are smooth. The function $\tilde{g}$ maps A_1^+ onto U^+ (an open set located outside the unitary disk) and A_1^- onto U^- (an open set located inside the unitary disk). Furthermore, the function $\tilde{g}|_{A^+ \cup A_1^-} : A_1^+ \cup A_1^- \to U^- \cup U^+$ is a conformal mapping. Consider next a conformal mapping ϕ which maps a neighborhood of z_1 onto a neighborhood of 0 as in Figure 5 and such that the image of the unitary circle is the imaginary axis. We can then apply [7, Theorem 16.8]: the function $\xi_0 \circ \tilde{g}^{-1} \circ \phi^{-1}$ is holomorphic on both sides of the imaginary axis and continuous across this boundary, so it is holomorphic over the whole domain. We deduce that ξ_0 is holomorphic across the boundary between A_1^+ and A_1^-. We can repeat this process with the domains $A_1^+ \cup A_2^-$, $A_2^+ \cup A_2^-$ and so on. Finally, we obtain that ξ_0 is holomorphic on the whole disk $D(z_0, R)$ except maybe at the point z_0. But once more, the continuity of the function ξ_0 does not allow this possibility. □

As already mentioned, the potential function can make some singularities of f^{-1} to vanish. This is illustrated by the example of Figure 6.

6.2 Asymptotic expansion of the holomorphic potential

In this section, we shall compute the asymptotic expansion of ξ in terms of the geometrical data of $\mathcal{S}_0$ and the configuration $(\mathbf{p}, \mathbf{v}) \in \mathcal{P} \times \mathcal{V}$. As explained in the preceding section, we know that if $\mathcal{S}_0$ is not one of the solid listed in Theorem 4.1, the potential function admits no analytic continuation on the whole complex plane. It allows one to deduce where is the solid approximately. For all $\nu \in \mathbf{C}$, we can next consider Γ, a contour large enough to encircle the solid and the point ν. The contour $\widetilde{\Gamma} := f(e^{-i\alpha}(\Gamma - r))$ encircles the unitary disk. According to the expression (1.1) of the

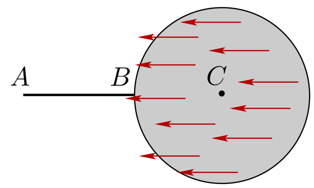

Figure 6: The solid consists in a disk of center C with a segment $[A, B]$. When this solid is moving to the left, parallel to the segment, one can easily check that the potential coincides with the potential of the disk. Although any analytic continuation of f^{-1} has singularities at A and B, the complex potential does not see these points. In this case, the singularities do not allow one to determine the orientation of the solid.

potential as a Laurent series, we obtain that, for all $n \geq 1$:

$$\begin{aligned}\lambda_n(\nu) = \frac{1}{2i\pi}\oint_\Gamma \xi(z)(z-\nu)^{n-1}\mathrm{d}z &= \frac{e^{i\alpha}}{2i\pi}\oint_{\widetilde{\Gamma}} \zeta(z)\left(e^{i\alpha}f(z)+r-\nu\right)^{n-1}f'(z)\mathrm{d}z\\ &= \frac{1}{n}\frac{1}{2i\pi}\oint_{\widetilde{\Gamma}}\zeta(z)\frac{d}{dz}\left(e^{i\alpha}f(z)+r-\nu\right)^{n}\mathrm{d}z\\ &= -\frac{1}{n}\frac{1}{2i\pi}\oint_{\widetilde{\Gamma}}\zeta'(z)\left(e^{i\alpha}f(z)+r-\nu\right)^{n}\mathrm{d}z\\ &= -\frac{1}{n}\frac{1}{2i\pi}\sum_{k=0}^{n}\binom{n}{k}e^{ik\alpha}(r-\nu)^{n-k}\oint_{\widetilde{\Gamma}}\zeta'(z)f(z)^k\mathrm{d}z.\end{aligned}$$

If we define the complex sequence $d := (d_k)_{k\in\mathbf{Z}}$ by $d_k := (k+1)\zeta_{k+1}$ for all $k \leq -1$ and $d_k = 0$ for $k \geq 0$, we obtain:

$$\lambda_n(\nu) = -\frac{1}{n}\sum_{k=1}^{n}\binom{n}{k}e^{ik\alpha}(r-\nu)^{n-k}(d*c^k)_{-1}, \quad (\nu\in\mathbf{C}).$$

We can rewrite the last term:

$$\begin{aligned}(d*c^k)_{-1} &= \sum_{i_1+\ldots+i_{k+1}=-1} c_{i_1}\ldots c_{i_k}d_{i_{k+1}}\\ &= -A_k\bar{w}_0 + B_k w_0 + i\omega C_k,\end{aligned}$$

where

$$A_k := \sum_{\substack{i_1+\ldots+i_{k+1}=0\\ i_1\leq -1}} i_1 c_{i_1}\ldots c_{i_{k+1}}, \qquad B_k := \sum_{\substack{i_1+\ldots+i_{k+1}=0\\ i_1\leq -1}} i_1\bar{c}_{-i_1}c_{i_2}\ldots c_{i_{k+1}},$$

$$C_k := \sum_{\substack{i_1+\ldots+i_{k+2}=0\\ i_1+i_2\leq -1}} (i_1+i_2)\bar{c}_{-i_1}c_{i_2}\ldots c_{i_{k+2}}.$$

In the following, to simplify the notation, we will rather consider the quantities $\mathcal{A}_k := -A_k/k$, $\mathcal{B}_k := -B_k/k$ and $\mathcal{C}_k := -C_k/k$. Indeed, we get, for all $n \geq 1$:

$$\lambda_n(\nu) = \sum_{k=1}^{n}\binom{n-1}{k-1}e^{ik\alpha}(r-\nu)^{n-k}\Big[-\mathcal{A}_k\bar{w}_0 + \mathcal{B}_k w_0 + i\omega\mathcal{C}_k\Big]. \qquad (6.2)$$

The problem of detection can now be reformulated as a purely algebraic problem: the complex sequence $(\lambda_j(\nu))_{j\geq 1}$ being given for all $\nu \in \mathbf{C}$, as well as the complex numbers $\mathcal{A}_k$, $\mathcal{B}_K$ and $\mathcal{C}_k$ ($k \geq 1$), can we solve the infinite nonlinear system of equations (6.2) and find the values of r, α, w_0 and ω? According to the results of both Section 2 and Section 4, we already know that there exist cases (namely, coefficients $(c_k)_{k\in\mathbf{Z}}$) for which the answer is negative.

In order to rewrite this infinite set of equations in a convenient short form, we introduce some linear operators: let us denote by N any positive integer and define $\mathcal{G}_N : \mathbf{R}^3 \to \mathbf{C}^N$ by $(\mathcal{G}_N U)_k := (-\mathcal{A}_k + \mathcal{B}_k)U_1 + i(\mathcal{A}_k + \mathcal{B}_k)U_2 + i\mathcal{C}_k U_3$ for all $U = (U_1, U_2, U_2)^T \in \mathbf{R}^3$ and all $1 \leq k \leq N$. We define $D_N : \mathbf{C}^N \to \mathbf{C}^N$ and $S_N : \mathbf{C}^N \to \mathbf{C}^N$ as well, by respectively $(D_N Z)_k := kZ_k$ ($1 \leq k \leq N$) and $(S_N Z)_1 := 0$ and $(S_N Z)_k := Z_{k-1}$ ($2 \leq k \leq N$) for all $Z := (Z_1, \ldots, Z_N) \in \mathbf{C}^N$. The first N equations (6.2) can now be rewritten as:

$$\Lambda_N(\nu) = e^{\log(r-\nu)D_N} e^{S_N D_N} e^{-\log(r-\nu)D_N} e^{i\alpha D_N} \mathcal{G}_N U, \tag{6.3a}$$

$$= \Theta_N(r-\nu, \alpha)\mathcal{G}_N U, \tag{6.3b}$$

where $U := (\Re(w_0), \Im(w_0), \omega)^T$ and $\Lambda_N(\nu) := (\lambda_1(\nu), \ldots, \lambda_N(\nu))^T$. The operator $e^{S_N D_N}$ is lower triangular and the identity $(e^{S_N D_N})_{k,n} = \binom{n-1}{k-1}$ for all $1 \leq k \leq n \leq N$, not so obvious, can be found in [2]. Considering the expressions (6.3), it is worth noticing that:

- In (6.3), the coefficients $\lambda_j(\nu)$ in the asymptotic expansion of ξ are obtained by applying to the vector U (the *velocity*) first the operator $\mathcal{G}_N$ encapsulating the information relating to the geometry of the solid and next the operator $\Theta_N(r-\nu, \alpha)$ depending only on the position.

- The linear operator $\mathcal{G}_N$ depends on the complex sequence c only, i.e. on the shape of the solid. Moreover, the complex quantities $\mathcal{A}_k - c_{-k}c_1^k$ ($k \geq 1$), $\mathcal{B}_{k+1} - c_{-k}\bar{c}_1 c_1^k$ ($k \geq 2$) and $\mathcal{C}_{k-1} - c_{-k}\bar{c}_{-1}c_1^{k-1}$ ($k \geq 1$) do not depend on c_{-n} for all $n \geq k$. In other words, for all $N \geq 1$, $\mathcal{G}_N$ depends on $c_1, c_{-1}, c_{-2}, \ldots, c_{-N-1}$ only. We deduce:

  Proposition 6.2. *Let $\mathcal{S}_0^1$ and $\mathcal{S}_0^2$ be two shapes described by means of the complex sequences $(c_k^1)_{k\geq 1}$ and $(c_k^2)_{k\geq 1}$, such that $c_k^1 = c_k^2$ for all $1 \leq k \leq N$. Then, if both solids have the same configuration, their complex potentials will have the same asymptotic expansion up to the order $N-1$.*

- The solutions $(r_1, r_2, \alpha, \Re(w_0), \Im(w_0), \omega)^T$ of all of the equations (6.3) (for all $N \geq 1$), form a subanalytic set of $\mathbf{R}^6$ (because Θ_N is analytic in r_1, r_2 and α). This subanalytic set has dimension d with $0 \leq d \leq 6$. However, because the dependence in $(\Re(w_0), \Im(w_0), \omega)^T$ is linear, if it had dimension $d \geq 4$, it would entail the existence of a position $(r_1, r_2, \alpha)^T$ and a non-zero velocity $U_0 \in \mathbf{R}^3$ such that $\Theta_N(r-\nu, \alpha)\mathcal{G}_N U_0 = 0$ for all $N \geq 1$. As already mentioned before, this case is only possible if the solid is in the list of Theorem 4.1.

  We do not know if there exist solids such that $0 < d \leq 3$. Observe that in Section 2, we have only given examples for which the solids can occupy a finite number of different positions, so $d = 0$ in these cases.

For all $N \geq 1$, we can invert the system (6.3) to obtain:

$$\mathcal{G}_N U = e^{-i\alpha D_N} e^{\log(r-\nu)D_N} e^{-S_N D_N} e^{-\log(r-\nu)D_N} \Lambda_N(\nu), \tag{6.4}$$

$$= \Theta_N(r-\nu, \alpha)^{-1}\Lambda_N(\nu), \tag{6.5}$$

or equivalently, with the notation of equation (6.2),

$$-\mathcal{A}_n\bar{w}_0+\mathcal{B}_nw_0+i\omega\mathcal{C}_n=e^{-in\alpha}\left[\sum_{k=1}^{n}\binom{n-1}{k-1}(\nu-r)^{n-k}\lambda_k(\nu)\right], \tag{6.6}$$

for all $n\in\mathbf{N}$. In this form, we can easily prove:

Proposition 6.3. *If the solid does not come out in Theorem 4.1 and its position is given, then we can deduce its velocity.*

Proof. Denote $\mathcal{G}^j$ $(j=1,2,3)$ the complex sequences respectively defined by $\mathcal{G}^1_k:=(-\mathcal{A}_k+\mathcal{B}_k)_{k\geq 1}$, $\mathcal{G}^2_k:=(i(\mathcal{A}_k+\mathcal{B}_k))_{k\geq 1}$ and $\mathcal{G}^3_k:=(i\mathcal{C}_k)_{k\geq 1}$. If these sequences were not $\mathbf{R}$-linearly independent in $\mathbf{C}^{\mathbf{N}}$, it would exist $(U_1,U_2,U_3)^T\neq 0$ in $\mathbf{R}^3$ such that $\sum_j U_j\mathcal{G}^j=0$ and then, for any position (r,α) and any $N\geq 1$, we would have $\Theta_N(r-\nu,\alpha)\mathcal{G}_NU=0$ which contradicts the assumption that the solid is not listed in Theorem 4.1. Conversely, if the sequences $\mathcal{G}^i$ are $\mathbf{R}$-linearly independent, then there exists $N_0\geq 3$ such that for all $N\geq N_0$, $\mathcal{G}_N$ is of rank 3 and the proof is completed. ☐

Proposition 6.4. *Assume that the shape $\mathcal{S}_0$ of the solid, described by the conformal mapping (3.1), is such that $e^{i\pi/2}\mathcal{S}_0=\mathcal{S}_0$ (the shape of the solid is invariant by rotation of angle $\pi/2$ and center 0). Then , from the holomorphic potential ξ, we can always deduce the values of r, $w_0e^{i\alpha}$ (the linear velocity expressed in a the reference fixed frame) and $|\omega|$ (the absolute value of the rotational velocity).*

Proof. The assumption on the shape $\mathcal{S}_0$ means that $f(\Omega)=\tilde{f}(\Omega)$ where $\tilde{f}$ is the conformal mapping defined by:

$$\tilde{f}(z):=\tilde{c}_1z+\sum_{k\leq 1}\tilde{c}_kz^k,\quad (z\in\Omega),$$

with $\tilde{c}_k=e^{i\pi/2}c_k$ for any $k=1$ and $k\leq -1$. Replacing the function f by $\tilde{f}$ in the computations, we obtain that:

$$\lambda_n(\nu)=\sum_{k=1}^{n}\binom{n-1}{k-1}e^{ik\alpha}(r-\nu)^{n-k}\Big[-\mathcal{A}_ke^{i(k+1)\pi/2}\bar{w}_0+\mathcal{B}_kw_0e^{i(k-1)\pi/2}+i\omega\mathcal{C}_ke^{ik\pi/2}\Big], \tag{6.7}$$

and the coefficients $\lambda_k(\nu)$, defined equivalently by (6.2) and by (6.7), must be equal for all $r,\nu\in\mathbf{C}$, $\alpha\in\mathbf{R}/2\pi$ and all $w_0\in\mathbf{C}$ and $\omega\in\mathbf{R}$. In particular, for $r=\nu=0$ and $\alpha=0$, we obtain that $\mathcal{A}_n(1-e^{i(n+1)\pi/2})w_0-\mathcal{B}_n(1-e^{i(n-1)\pi/2})\bar{w}_0=0$ and $\mathcal{C}_n(1-e^{in\pi/2})\omega=0$ for all $w_0\in\mathbf{C}$, $\omega\in\mathbf{R}$ and $n\geq 1$. We deduce that $(\mathcal{A}_n\neq 0)\Leftrightarrow(n\equiv -1\ [4])$, $(\mathcal{B}_n\neq 0)\Leftrightarrow(n\equiv 1\ [4])$ and $(\mathcal{C}_n\neq 0)\Leftrightarrow(n\equiv 0\ [4])$.

Let us consider the problem of detection now we got some extra information about $\mathcal{A}_n$, $\mathcal{B}_n$ and $\mathcal{C}_n$. Equation (6.6) with $n=2$, gives $\lambda_1(\nu-r)+\lambda_2(\nu)=0$ for all $\nu\in\mathbf{C}$. Two cases have to be considered:

- Either $\lambda_1=0$, which means also that $\lambda_2(\nu)=0$ for all $\nu\in\mathbf{C}$. It entails, according to equation (6.6) with $n=1$, that $\mathcal{B}_1w_0=0$. But $\mathcal{B}_1=|c_1|^2\neq 0$ and hence $w_0=0$. We get $\omega\neq 0$ otherwise we would have $\xi=0$. Let now m be the smallest index such that $\mathcal{C}_m\neq 0$. We know that such an index exists, otherwise it would mean that $\mathcal{C}_k=0$ for all $k\geq 1$ and hence that any rotational motion of the solid generates a complex potential equal to 0. This is impossible for solid not listed in Theorem 4.1. By induction on n with equation (6.6), we must have now $\lambda_n(\nu) = 0$ for all $n < m$. We use then equation (6.6) with $n = m$ to obtain $i\omega\mathcal{C}_m = e^{-im\alpha}\lambda_m(\nu)$ and next equation (6.2) with $n = m + 1$ to get $\lambda_{m+1}(\nu) = me^{im\alpha}(r - \nu)i\omega\mathcal{C}_m$. Combining these two identities, we eventually obtain $\lambda_{m+1}(\nu) = m\lambda_m(\nu)(r - \nu)$, whence we deduce the value of r.

- Or $\lambda_1 \neq 0$. In this case, we deduce easily the value of r from the relation $\lambda_1(\nu - r) + \lambda_2(\nu) = 0$.

Then, equation (6.6) with $n = 1$ gives us the value of $w_0 e^{i\alpha}$. There exists at least one $m > 0$ such that $\mathcal{C}_m \neq 0$. Once again, equation (6.6) with $n = m$ allows us to deduce the value of $|\omega|$. □

If we have more information on $\mathcal{S}_0$, we can go further in our study:

Proposition 6.5. *In the preceding proposition, assume furthermore that one of the following assumption is satisfied:*

1. $w_0 \neq 0$ *and there exists an integer* m *such that either* $\mathcal{A}_m$ *and* $\mathcal{A}_{m+4}$ *or* $\mathcal{B}_m$ *and* $\mathcal{B}_{m+4}$ *are both different from 0;*

2. $\omega \neq 0$ *and there exists an integer* m *such that* $\mathcal{C}_m$ *and* $\mathcal{C}_{m+4}$ *are both different from* 0*;*

Then, the solid is detectable.

Proof. We know that we can compute r and $w_0 e^{i\alpha}$. Assume for instance that the second assumption holds (it would be the same reasoning with the first one). In this case, with equation (6.6) specifying $n = m$ and $n = m + 4$, we can compute $\omega e^{im\alpha}$ and $\omega e^{i(m+4)\alpha}$. We next deduce $e^{i4\alpha}$ and hence the orientation of the solid (because of the symmetry property, $e^{i4\alpha}$ suffices to provide the orientation). Since $m \equiv 0$ [4] (because $\mathcal{C}_m \neq 0$) we next deduce the values of $e^{im\alpha}$ and ω. We know that there exists at least one index p such that $\mathcal{A}_p \neq 0$. We use equation (6.6) with $n = p$ to deduce the value of $\mathcal{A}_p \bar{w}_0 e^{ip\alpha}$ or equivalently $\bar{\mathcal{A}}_p w_0 e^{-ip\alpha}$. Since necessarily $p \equiv -1$ [4] then $-p \equiv 1$ [4] and we can deduce the values of both ω and $e^{i4\alpha}$ with $w_0 e^{i\alpha}$. □

To conclude this section, we give examples of solids without any symmetry, which are detectable (one is pictured in Figure 7):

6.3 Example of detection

We consider a shape $\mathcal{S}_0$ described by a complex sequence c such that $c_1 \neq 0$, $c_{-4} \neq 0$ and $c_{-7} \neq 0$, all the other coefficients c_k being null. Direct computations lead to:

k	1	2	3	4	5	6	7	8
$\mathcal{A}_k$	0	0	0	$c_1^4 c_{-4}$	0	0	$c_1^7 c_{-7}$	0
$\mathcal{B}_k$	$\|c_1\|^2$	0	0	0	0	$\|c_1\|^2 c_1^4 c_{-4}$	0	0
$\mathcal{C}_k$	0	0	$c_1^3 \bar{c}_{-4} c_{-7}$	0	$2\|c_1\|^2 c_1^4 c_{-4}$	0	0	$(2\|c_1\|^2 + 3\|c_{-4}\|^2) c_1^7 c_{-7}$

Plugging these results into System (6.6), we obtain that:

$$\mathcal{B}_1 w_0 = e^{-i\alpha}\lambda_1, \tag{6.8a}$$
$$0 = e^{-i2\alpha}[\lambda_1(\nu - r) + \lambda_2(\nu)], \tag{6.8b}$$
$$\mathcal{C}_3 i\omega = e^{-i3\alpha}\left[\sum_{k=1}^{3}\binom{n-1}{k-1}(\nu - r)^{n-k}\lambda_k(\nu)\right], \tag{6.8c}$$
$$-\mathcal{A}_4 \bar{w}_0 = e^{-i4\alpha}\left[\sum_{k=1}^{4}\binom{n-1}{k-1}(\nu - r)^{n-k}\lambda_k(\nu)\right]. \tag{6.8d}$$

- If $\omega \neq 0$ and $w_0 \neq 0$: From equation (6.8a) we deduce that $\lambda_1 \neq 0$ and from (6.8b) we deduce the value of r. Equation (6.8c) allows us to determine $|\omega|$ and 3α up to π. Combining next equation (6.8a) and (6.8d), we get 5α. Using Bezout's relation: $\alpha = u3\alpha + v5\alpha$ with $u = 2$ and $v = -1$, we get α. We determine w_0 with equation (6.8a) and ω with equation (6.8c).

- if $\omega = 0$, $w_0 \neq 0$: We compute r as in the preceding case. Then, we need further calculations:

$$\mathcal{B}_6 w_0 = e^{-i6\alpha}\left[\sum_{k=1}^{6}\binom{n-1}{k-1}(\nu - r)^{n-k}\lambda_k(\nu)\right], \tag{6.9a}$$
$$-\mathcal{A}_7 \bar{w}_0 = e^{-i7\alpha}\left[\sum_{k=1}^{7}\binom{n-1}{k-1}(\nu - r)^{n-k}\lambda_k(\nu)\right]. \tag{6.9b}$$

  With (6.9a) and (6.8a) we get 5α and with (6.9b) and (6.8a) we get 8α. Since 5 and 8 are coprime numbers, we deduce the value of α. We conclude as in the preceding case.

- If $\omega \neq 0$ and $w_0 = 0$: With (6.8a) and (6.8b) we deduce that $\lambda_1 = \lambda_2(\nu) = 0$ for all $\nu \in \mathbf{C}$. We rewrite (6.8c) and (6.8d) as

$$\mathcal{C}_3 i\omega = e^{-i\alpha}\lambda_3,$$
$$0 = \lambda_4(\nu) + 3(\nu - r)\lambda_3,$$

  and we deduce first that $\lambda_3 \neq 0$ and then the value of r. We next add the equations:

$$\mathcal{C}_5 i\omega = e^{-i5\alpha}\left[\sum_{k=1}^{5}\binom{n-1}{k-1}(\nu - r)^{n-k}\lambda_k(\nu)\right], \tag{6.10a}$$
$$\mathcal{C}_8 i\omega = e^{-i8\alpha}\left[\sum_{k=1}^{5}\binom{n-1}{k-1}(\nu - r)^{n-k}\lambda_k(\nu)\right]. \tag{6.10b}$$

  Equations (6.8c) and (6.10a) give us 2α and (6.10a) and (6.10b) give us 3α. Since 2 and 5 are coprime numbers we get α and next ω with (6.8c).

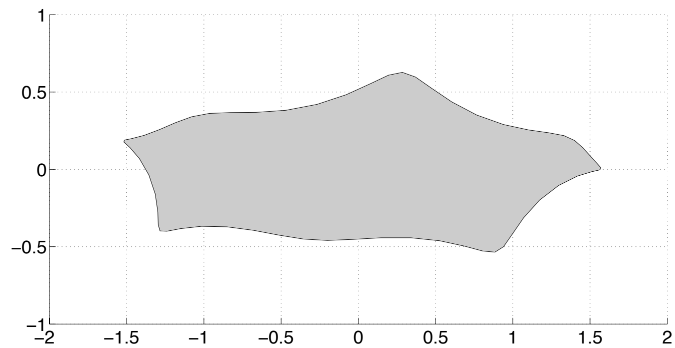

Figure 7: Example of detectable solid as described in Subsection 6.3.

7 Tracking

In this Section, we perform the proof of Theorem 1.4. So we assume that we know the complex potential for all t in a time interval $[0,T]$ $(T>0)$. For all $t\in[0,T]$, we have an expression

$$\xi(t,z):=\sum_{j\geq 1}\frac{\lambda_j(t,\nu)}{(z-\nu)^j},\quad |z-\nu|>R(t,\nu), \tag{7.1}$$

where $\lambda_j(t,\nu)$ are complex numbers and $R(t,\nu):=\limsup_{j\to+\infty}|\lambda_j(t,\nu)|^{1/j}$. At any time t, the series is uniformly convergent on $\{z\in\mathbf{C}\,:\,|z-\nu|>R(t,\nu)\}$. For all $N\geq 1$, we denote $\Lambda_N(t,\nu):=(\lambda_1(t,\nu),\ldots,\lambda_N(t,\nu))^T$ and we have, according to the results of the preceding section:

$$\mathcal{G}_N U(t)=\Theta_N(r(t)-\nu,\alpha(t))^{-1}\Lambda_N(t,\nu),$$

where we recall that $U(t):=(\Re(w_0(t)),\Im(w_0(t)),\omega(t))^T$. In the proof of Proposition 6.3 we have shown that if the solid is not one of those described in Theorem 4.1, then there exists $N\geq 1$ such that $\mathcal{G}_N$ has rank 3. It means that there exists (at least) one inverse $\mathcal{G}_N^{-1}$ allowing one to express the velocity as:

$$U(t):=\mathcal{G}_N^{-1}\Theta_N(r(t)-\nu,\alpha(t))^{-1}\Lambda_N(t,\nu).$$

We next get:

$$\begin{pmatrix} e^{i\alpha(t)}w_0(t)\\ \omega\end{pmatrix}=\begin{pmatrix} e^{i\alpha(t)} & ie^{i\alpha(t)} & 0\\ 0 & 0 & 1\end{pmatrix}\mathcal{G}_N^{-1}\Theta_N(r(t)-\nu,\alpha(t))^{-1}\Lambda_N(t,\nu).$$

This equation can be rewritten as:

$$\frac{d}{dt}\begin{pmatrix} r(t)\\ \alpha(t)\end{pmatrix}=\begin{pmatrix} e^{i\alpha(t)} & ie^{i\alpha(t)} & 0\\ 0 & 0 & 1\end{pmatrix}\mathcal{G}_N^{-1}\Theta_N(r(t)-\nu,\alpha(t))^{-1}\Lambda_N(t,\nu),$$

to which we can apply the Cauchy-Lipschitz Theorem. The proof is then completed.

8 Conclusion

In this article, we have proved that not all the solids moving in a perfect fluid are detectable by measuring the potential of the fluid. This observation has led us to define the notion of *detectable* solids, which is a purely geometric property. When the geometry was described by means of a conformal mapping, we were able to exhibit examples of detectable (or partially detectable) solids. However, the complete characterization of such solids in terms of the complex sequence $(c_k)_{k\in\mathbf{Z}}$ remains to be done.

References

[1] C. Alvarez, C. Conca, L. Friz, O. Kavian, and J. H. Ortega. Identification of immersed obstacles via boundary measurements. *Inverse Problems*, 21(5):1531–1552, 2005.

[2] G. S. Call and D. J. Velleman. Pascal's matrices. *Amer. Math. Monthly*, 100(4):372–376, 1993.

[3] C. Conca, P. Cumsille, J. Ortega, and L. Rosier. On the detection of a moving obstacle in an ideal fluid by a boundary measurement. *Inverse Problems*, 24(4):045001, 18, 2008.

[4] A. Doubova, E. Fernández-Cara, and J. H. Ortega. On the identification of a single body immersed in a Navier-Stokes fluid. *European J. Appl. Math.*, 18(1):57–80, 2007.

[5] H. Heck, G. Uhlmann, and J.-N. Wang. Reconstruction of obstacles immersed in an incompressible fluid. *Inverse Probl. Imaging*, 1(1):63–76, 2007.

[6] L. M. Milne-Thomson. *Theoretical hydrodynamics.* 4th ed. The Macmillan Co., New York, 1960.

[7] W. Rudin. *Real and complex analysis.* McGraw-Hill Book Co., New York, third edition, 1987.